Aly Abdelmagid, Zlata Tošić, Anahita Mirani, Ahmed Hussein, Ahmed Elshafei

Design Model for Block-Based Structures from Triply Orthogonal Systems of Surfaces

Abstract: A design model for structures constituted by a system of planar blocks based on the geometry of Triply Orthogonal Systems of Surfaces (TOS) is presented. This model goes from the different TOS types generated together with preserving Möbius transformation to the blocks' assembly and sizing. Based on the design model, a prototype for a TOS version of the topological interlocking system is explored.

1 Introduction

Triply Orthogonal Systems of Surfaces (TOS) take the geometric advantages of principal patches, in particular, generating planar faces (up to architectural tolerance) cf. (Bobenko and Tsarev 2007), (Liu et al. 2006) and establishing them in a three dimensional setting cf. (Abdelmagid et al. 2022). A TOS can be parameterized by three mutually-orthogonal families of principal patches, giving rise to a 3D array of points generating a 3D array of blocks, as seen in the Figure 1. The system of TOS blocks in question is useful in the fabrication of structures made by assembling blocks in an array of one, two, or three dimensions. In this context, we present a design model for block-based structures arising from the geometry of TOS. More precisely, we use three ways of generating TOS by differential-geometric methods, as well as constructing their Möbius transformations which preserve their TOS structures. Furthermore, we show how the TOS can generate a version of the topological interlocking system (based on regular tessellations of space) for stereotomy of stone vaults cf. (Brocato and Mondardini 2010) to an interlocking system based on irregular tessellations of space with TOS blocks made out of planar faces while maintaining their construction principles and the planarity of the contact faces between the blocks.

2 Geometry

To begin let us briefly recall some results from differential geometry, for more extensive reading check (Eisenhart 1909) and (Gray et al. 2006).

https://doi.org/10.1515/9783111162683-013

2.1 TOS generating three-dimensional array of points

A triply orthogonal system of surface on an open set $\mathcal{U} \subset \mathbb{R}^3$ consists of three families $\mathcal{R}, \mathcal{G}, \mathcal{B}$ of surfaces that intersect each other orthogonally. More concretely, we think of a TOS as a curvilinear coordinates system arising from a smooth three-dimensional patch $X(u, v, w)$ satisfying the mutual orthogonality condition (with respect to the Euclidean scalar product $\langle , \rangle$ on $\mathbb{R}^3$) given by

$$\langle X_u, X_v \rangle = 0 \quad , \quad \langle X_v, X_w \rangle = 0 \quad , \quad \langle X_w, X_u \rangle = 0. \tag{1}$$

We recall that by the theorem of Dupin, the curves of intersections of the surfaces in a TOS patch X are principal curves on the surfaces in question. In other words, for fixed parameters u_o, v_o, w_o the two-dimensional patches R, G, B defined by

$$R(v, w) = X(u_o, v, w) \quad , \quad G(w, u) = X(u, v_o, w) \quad , \quad B(u, v) = X(u, v, w_o)$$

are all the so-called principal patches. These are known to be the continuous smooth analogues of circular planar quadrilateral meshes cf. (Liu et al., 2006). This means that by evaluating the continuous smooth TOS patch $X(u, v, w)$ at discrete values of u, v, w we obtain a three-dimensional array of discrete points whose (quadrilateral) faces are all planar (up to architectural tolerance) cf. (Bobenko and Tsarev 2007), as seen in Fig. 1.

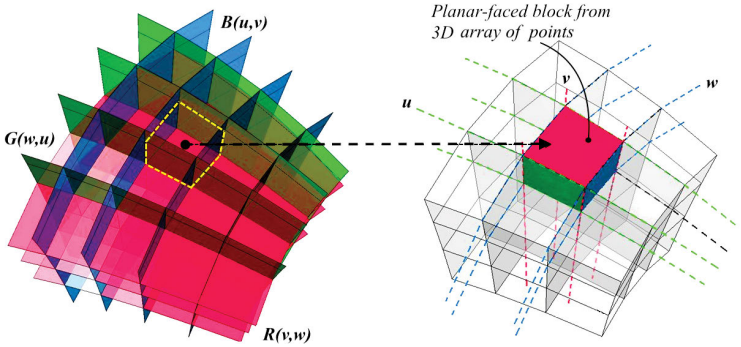

Fig. 1: R, G, B principal patches inducing a 3D array of points forming blocks with planar faces.

2.2 Generating TOS

A known result of Darboux states that the determination of a general TOS amounts to solving partial differential equations of the third order called the Lamé system (Eisenhart 1909). A solution consists of the (unitary) tangent vector fields to the TOS which

are further integrated to obtain the patch X. However, we use here three differential-geometric constructions of TOS bypassing the Lamé system and giving us explicit TOS patch parameterizations as follows.

TOS from Quadrics: This TOS type is explained by the authors (Abdelmagid et al. 2022).

TOS from DOS: The second TOS type's construction is based on revolving or extruding a Doubly Orthogonal System of Curves (DOS) which is given as a principal patch $B(u, v)$ in the plane or space. In the revolving case, B is a portion of the plane $\mathbb{R}^2$ which is then rotated about an axis l with angle w giving the third coordinate. In the extrusion case, B defines a surface in $\mathbb{R}^3$, which is then extruded along its normals N with offset distance w giving the third coordinate. Denoting by ρ the rotation matrix in question, then the TOS patches are given by

$$\text{Revolving:}\quad X(u, v, w) = \rho(l, w) \cdot B(u, v) \tag{2}$$

$$\text{Extruding:}\quad X(u, v, w) = B(u, v) + wN(u, v). \tag{3}$$

The TOS from revolving DOS has its $\mathcal{B}$ family planar and its $\mathcal{R}$, $\mathcal{G}$ families surfaces of revolution, as seen in Fig. 2a, while the TOS from extruding DOS, has its $\mathcal{B}$ family all offsets of B and its $\mathcal{R}$, $\mathcal{G}$ families all developable surfaces (and in some cases planar), as seen in Fig. 2b.

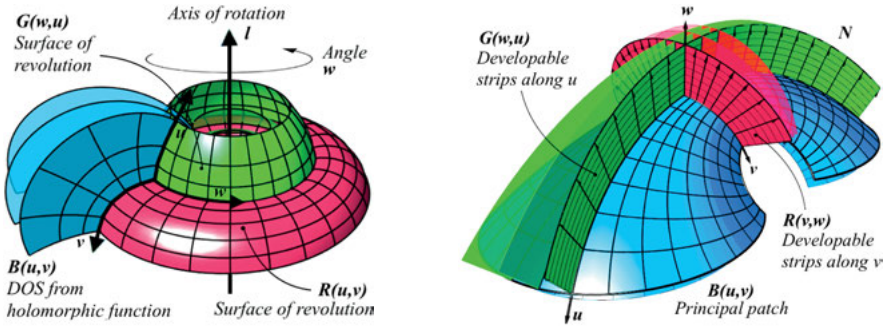

Fig. 2: TOS arising from DOS: (a) TOS from revolving DOS, (b) TOS from extruding DOS.

We will focus in particular on planar DOS patches $B(u, v)$ arising from (regular) holomorphic functions $f(z)$ defined on (an open subset of) the complex plane. This is following from the fact that such a function f is conformal (i. e. preserves angles). This is seen in the planar DOS patch $B(u, v)$ in Fig. 2a which is defined by the real and imaginary parts of a holomorphic function $f(z)$ that is

$$B(u, v) = (\Re f(z), \Im f(z)) \quad , \quad z = u + iv \in \mathcal{U} \subset \mathbb{C} \simeq \mathbb{R}^2. \tag{4}$$

TOS from Bianchi Transforms: In this TOS type, the $\mathcal{B}$ family are surfaces of negative constant Gaussian curvature (CGC) $-1/\rho^2$ with $\rho > 0$, also known as the TOS of Ribaucour cf. (Eisenhart 1909). This follows from a theorem of Ribaucour stating that if $F(u, v)$ is a surface of negative CGC $-1/\rho^2$ then the circles in the tangent planes at points $p \in F$ of radius ρ are the orthogonal trajectories of a family $\mathcal{B}$ of surfaces of negative CGC $-1/\rho^2$, as seen in Fig. 3a. It turns out that family $\mathcal{B}$ can be realized from the Bianchi transformation of the negative CGC surface F. To see this, we assume that $F(u, v)$ is a Tchebyshef principal patch of angle function $\theta(u, v)$ cf. (Gray et al. 2006). Next, finding a solution $\theta^*(u, v, w)$ to the Bianchi-Darboux equations

$$\begin{cases} \theta^*_u + \theta_v = \sin\theta^* \cos\theta \\ \theta^*_v + \theta_u = -\cos\theta^* \sin\theta \end{cases} \tag{5}$$

where the constant of integration denoted w will provide the third coordinate in the TOS, parameterizing the circles orthogonal to the $\mathcal{B}$ family, as seen in Fig. 3a. Finally, the TOS patch X in question is defined by the Bianchi transformation

$$X(u, v, w) = F(u, v) + \left(\frac{\cos(\theta^*(u, v, w))}{\cos(\theta(u, v))}\right) F_u + \left(\frac{\sin(\theta^*(u, v, w))}{\sin(\theta(u, v))}\right) F_v \tag{6}$$

where for every fixed w_o we have a negative CGC surface $B(u, v) = X(u, v, w_o)$ which is a Bianchi transform of $F(u, v)$, while F itself is not part of the TOS.

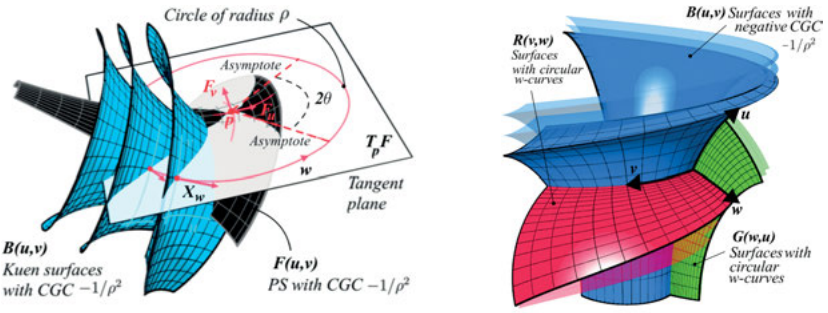

Fig. 3: TOS of Ribaucour from Bianchi transformation: (a) $\mathcal{B}$ family orthogonal to circles, (b) $\mathcal{B}$ surfaces of negative CGC.

2.3 Möbius transformations of the TOS

We will now show how to transform the TOS patches to obtain other TOS patches, using the so-called Möbius transformation. The fact that Möbius transformations preserve TOS patches follows from their preservation of principal patches, a result due to Darboux cf. (Eisenhart 1909). Intuitively, Möbius transformations are constructed from

compositions of reflections and inversions. However, for convenience of application, albeit less intuitive we construct them as Lorentz transformations preserving a light cone in Minkowski space $\mathbb{R}^{4,1}$ and composed with the stereographic projection cf. (Cecil 2018), as seen in Fig. 4.

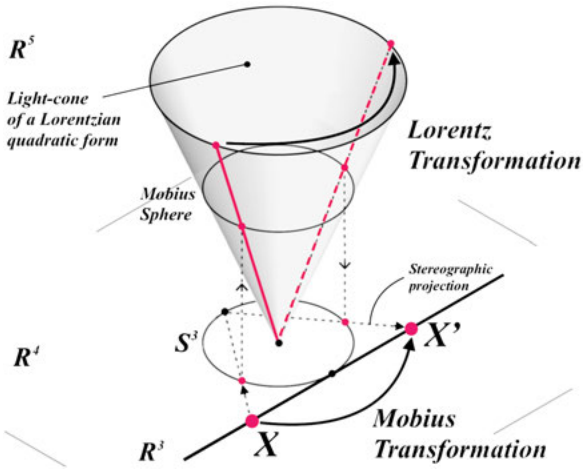

Fig. 4: Möbius transformation as Lorentz transformation.

Thanks to this construction, a Möbius transformation is given by a 5×5 matrix

$$\mu = A^k(\mathfrak{a}) \cdot B^l(\mathfrak{b}) \cdot C^m(\mathfrak{c}) \cdot D^n(\mathfrak{d}) \tag{7}$$

$$A(\mathfrak{a}) = \begin{pmatrix} \frac{1}{\sqrt{1-\mathfrak{a}^2}} & 0 & 0 & 0 & -\frac{\mathfrak{a}}{\sqrt{1-\mathfrak{a}^2}} \\ 0 & 1 & 0 & 0 & 0 \\ 0 & 0 & 1 & 0 & 0 \\ 0 & 0 & 0 & 1 & 0 \\ -\frac{a}{\sqrt{1-\mathfrak{a}^2}} & 0 & 0 & 0 & \frac{1}{\sqrt{1-\mathfrak{a}^2}} \end{pmatrix} \quad B(\mathfrak{b}) = \begin{pmatrix} 1 & 0 & 0 & 0 & 0 \\ 0 & \frac{1}{\sqrt{1-\mathfrak{b}^2}} & 0 & 0 & -\frac{\mathfrak{b}}{\sqrt{1-\mathfrak{b}^2}} \\ 0 & 0 & 1 & 0 & 0 \\ 0 & 0 & 0 & 1 & 0 \\ 0 & -\frac{\mathfrak{b}}{\sqrt{1-\mathfrak{b}^2}} & 0 & 0 & \frac{1}{\sqrt{1-\mathfrak{b}^2}} \end{pmatrix}$$

$$C(\mathfrak{c}) = \begin{pmatrix} 1 & 0 & 0 & 0 & 0 \\ 0 & 1 & 0 & 0 & 0 \\ 0 & 0 & \frac{1}{\sqrt{1-\mathfrak{c}^2}} & 0 & -\frac{c}{\sqrt{1-\mathfrak{c}^2}} \\ 0 & 0 & 0 & 1 & 0 \\ 0 & 0 & -\frac{\mathfrak{c}}{\sqrt{1-\mathfrak{c}^2}} & 0 & \frac{1}{\sqrt{1-\mathfrak{c}^2}} \end{pmatrix} \quad D(\mathfrak{d}) = \begin{pmatrix} 1 & 0 & 0 & 0 & 0 \\ 0 & 1 & 0 & 0 & 0 \\ 0 & 0 & 1 & 0 & 0 \\ 0 & 0 & 0 & \frac{1}{\sqrt{1-\mathfrak{d}^2}} & -\frac{\mathfrak{d}}{\sqrt{1-\mathfrak{d}^2}} \\ 0 & 0 & 0 & -\frac{\mathfrak{d}}{\sqrt{1-\mathfrak{d}^2}} & \frac{1}{\sqrt{1-\mathfrak{d}^2}} \end{pmatrix}$$

with k, l, m, n integers and parameters $\mathfrak{a}, \mathfrak{b}, \mathfrak{c}, \mathfrak{d}$ of norm less than one, applied to a TOS patch X seen as an element of the light cone, as seen in Fig. 4.

3 Design model

Now that the geometric constructions are defined, the following part establishes a design model based on these constructions. In essence, the model takes the form of a series of choices induced by the geometric constructions, that we will call Degrees of Design Freedom (DF). Through the five DF, the designer goes from defining the global shape to its detailing on the block level.

3.1 DF-1 TOS-type

The TOS-types are interpreted as morphological choices. And they are classified as follows:

- **A01 and A02:** TOS Quadrics (Elliptic) and TOS Quadrics (Parabolic)
- **B01 and B02-(a,b):** TOS from DOS (Revolving) and TOS from DOS (Extruding)
- **C01:** TOS from Kuen (Bianchi transform).

3.2 DF-2 Variants

Each TOS-type contains within it a spectrum of variants that are controlled firstly by the coordinates u, v, w and secondly by parameters a, b, c, .. involved in the expression of the TOS patch X of each TOS-type. The coordinates u, v, w determine the surface choice in the families $\mathcal{R}$, $\mathcal{G}$, $\mathcal{B}$, while the parameters a, b, c, .. determine the shape of the TOS-type. Below, is a selection of examples.

B01: TOS-type is Revolving DOS obtained from considering the holomorphic function $f(z)$ (on an appropriate part of the complex plane) of the form

$$f(z) = \frac{(a_1 + ia_2)z + (b_1 + ib_2)}{(c_1 + ic_2)z + (d_1 + id_2)}$$

and inducing the DOS $B(u, v) = (r(u, v), s(u, v))$ given by

$$r = \frac{a_2d_1u - a_1d_2u + a_2c_1u^2 - a_1c2u^2 + a_1d_1v + a_2d_2v + a_2c_1v^2 - a_1c_2v^2 - b_1(d_2+c_2u+c_1v) + b_2(d_1+c_1u-c_2v)}{\left(d_1^2 + d_2^2 + 2d_2(c_2u + c_1v) + 2d_1(c_1u - c_2v) + (c_1^2 + c_2^2)(u^2 + v^2)\right)}$$

$$s = \frac{a_1d_1u + a_2d_2u + a_1c_1u^2 + a_2c_2u^2 - a_2d_1v + a_1d_2v + a_1c_1v^2 + a_2c_2v^2 + b_2(d_2+c_2u+c_1v) + b_1(d_1+c_1u-c_2v)}{\left(d_1^2 + d_2^2 + 2d_2(c_2u + c_1v) + 2d_1(c_1u - c_2v) + (c_1^2 + c_2^2)(u^2 + v^2)\right)}$$

The DOS is then revolved around an axis l with rotation parameter w and the variants are obtained by varying a_1, a_2, b_1, b_2, c_1, c_2, d_1, d_2 as seen in Fig. 5.

B02-b: TOS-type is Extruding DOS obtained from considering a principal patch which is a Dupin cyclide (elliptic type) given by the parameterization

$$\left(\frac{b\sin(2\pi u)(a - d\cos(2\pi v))}{a - c\cos(2\pi u)\cos(2\pi v)}, \frac{b\sin(2\pi v)(c\cos(2\pi u) - d)}{a - c\cos(2\pi u)\cos(2\pi v)}, -\frac{d(c - a\cos(2\pi u)\cos(2\pi v)) + b^2\cos(2\pi u)}{a - c\cos(2\pi u)\cos(2\pi v)}\right)$$

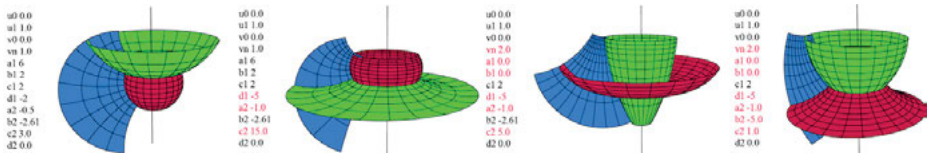

Fig. 5: Variants of TOS-type B01 (Revolving DOS).

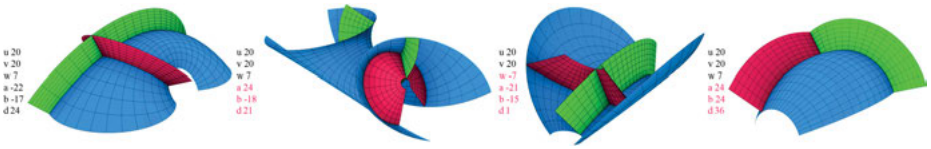

Fig. 6: Variants of B02: TOS from DOS (Extruding).

with $0 < b \leq a$ and $c^2 = a^2 - b^2$. The TOS is then generated by extruding this DOS along the normals with extrusion parameter w and the variants are obtained by varying the parameters a, b, c, d as seen in Fig. 6.

C01: TOS-type is Bianchi transform obtained from considering a Pseudo-Sphere (PS) that is parameterized by a Tchebyshef principal patch $F(u, v)$ with its angle function $\theta(u, v)$ given by

$$F(u,v) = \left(\frac{\cos v}{\cosh u}, \frac{\sin v}{\cosh u}, u - \tanh u\right) \quad , \quad \theta(u,v) = 2\arctan\left(e^u\right).$$

Next, solving the Bianchi-Darboux Equations (5) we obtain a one-parameter family of solutions $\theta^*(u, v, w)$ with parameter w (constant of integration) given by

$$\theta^*(u,v,w) = 2\arctan\left(\frac{-v-w}{\cosh u}\right).$$

Finally, putting everything in Bianchi transform Expression (6) we obtain a family of Kuen surfaces $B(u, v)$ forming a TOS patch $X(u, v, w)$ and where the w-curves shared by the $\mathcal{R}$, $\mathcal{G}$ surfaces are circular arcs as seen in Fig. 7

$$X = \rho\left(\frac{2(\cos v + (v+w)\sin v)\cosh u}{(v+w)^2 + \cosh^2 u}, \frac{2(\sin v - (v+w)\cos v)\cosh u}{(v+w)^2 + \cosh^2 u}, u - \frac{\sinh(2u)}{(v+w)^2 + \cosh^2 u}\right).$$

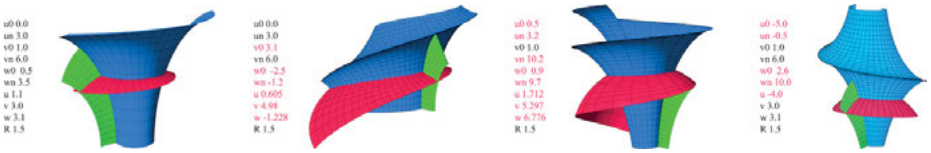

Fig. 7: TOS-type C01 (Bianchi transform).

3.3 DF-3 Möbius transformations

Möbius transformations expand even further the variety of morphological solutions while maintaining the structure of their associated TOS. A Möbius transformation μ given by the Expression (7) allows two-level manipulations. First, by different combinations of the generators A, B, C, D to obtain words of the form $AABCACD\ldots$ and second, by varying the parameters $\mathfrak{a}, \mathfrak{b}, \mathfrak{c}, \mathfrak{d}$. Selected examples of the application of Möbius transformations on some TOS-types are seen in Fig. 8.

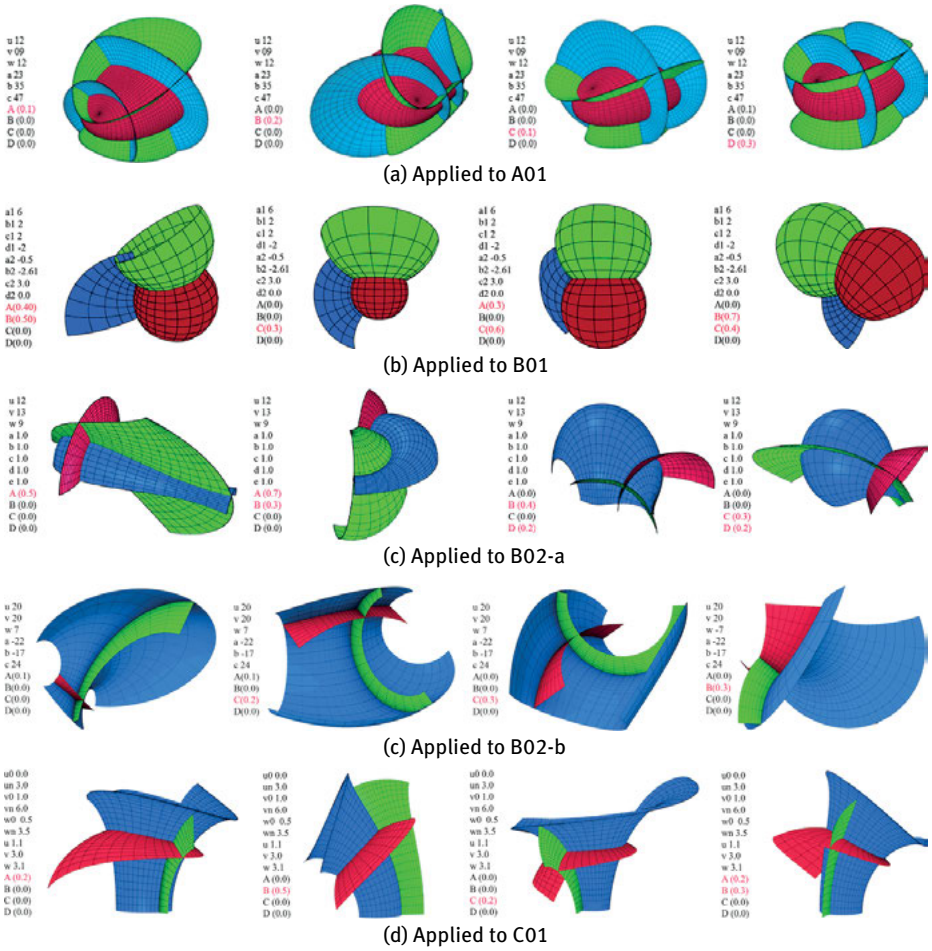

(a) Applied to A01

(b) Applied to B01

(c) Applied to B02-a

(c) Applied to B02-b

(d) Applied to C01

Fig. 8: Selected examples of Möbius transformation to some TOS-types.

3.4 DF-4 Blocks assembly

As explained above, any of the TOS-types creates a 3D array of points by evaluating the TOS patch X at discrete values of u, v, w, thus creating blocks with planar faces (see Fig. 1). It then follows naturally that DF-4 is the manner of assembling these blocks, namely, in arrays of one, two or three dimensions (Fig. 9). In particular, we observe that the 3D array offers a (non-regular) tessellation of (part of) $\mathbb{R}^3$, as seen in Fig. 9c.

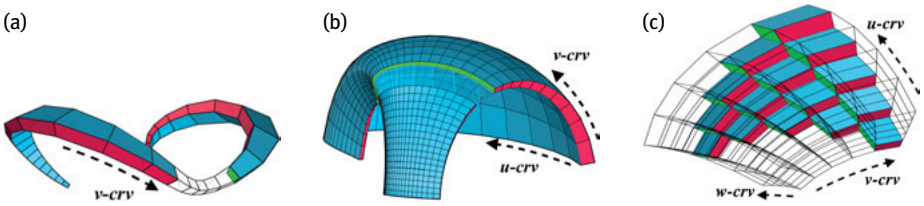

Fig. 9: Three fundamental types of blocks assembling: (a) 1D array, (b) 2D array and (c) 3D array.

3.5 DF-5 Blocks Sizing

This DF provides a way to control the sizes of the blocks arising from the TOS patch X using a reparameterization of the form $Y(x, y, z) = X(u(x), v(y), z(w))$ where $u(x)$, $v(y)$, $w(z)$ are the inverses of the functions $x(u)$, $y(v)$, $z(w)$. In Fig. 10, we can see how these functions control the block sizes by altering both the lengths of the u, v, w-domains and the step sizes of their discrete values. The option to size the blocks while maintaining their geometric properties provides the designer with a rationalized way to optimize material use and fabrication time.

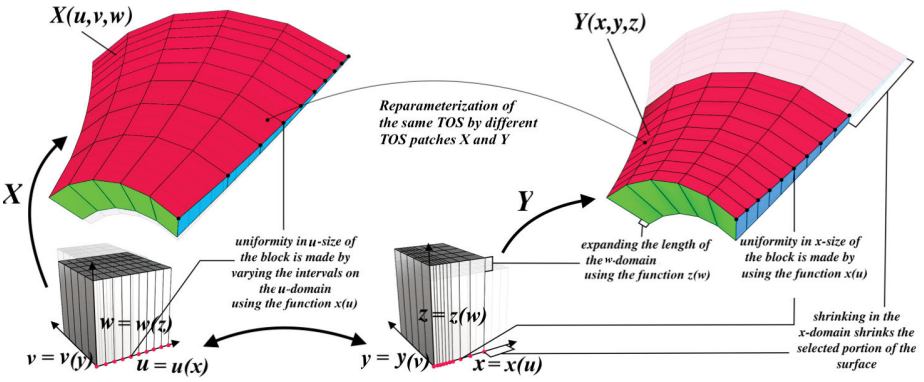

Fig. 10: Controlling blocks size through reparameterization.

4 Design application (TOS stone vault)

Next, we present a stone vault prototype based on an interlocking system of blocks arising from the TOS-type A01 3D array of points. The continuous nature of the TOS patch $X(u, v, w)$ allows us to generate an "intermediate" step size for the discrete blocks providing an overlapping version of the TOS 3D array which ensures planar contact faces between the blocks.

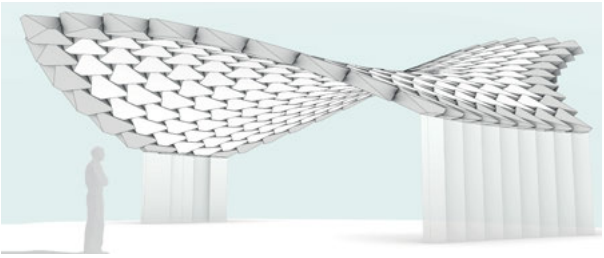

Fig. 11: Model of the TOS stone vault

Recall that TOS 3D points-array generate an irregular aperiodic tessellation of $\mathbb{R}^3$ where, the TOS blocks are neither platonic solids nor repeating. Nevertheless, they follow the structural principles of the classical interlocking system cf. (Brocato and Mondardini, 2010). More precisely, the mutual bearing between the blocks that are held together by a peripheral constraint as seen in Fig. 11.

TOS interlocking system

Observe that the overlapping of the planar contact faces between the blocks is achieved by using two-step sizes, namely, unit TOS blocks and big TOS blocks (clusters of 8 units). That means that each big TOS block is made out of 24 peripheral planar faces as seen in Fig. 12.

Even though having as many faces in a big TOS block is structurally sound, it is generally not ideal for fabrication, where it is naturally preferred to have the least amount of faces to cut. Notice that the 24 faces can be reduced to 6 faces per block by selecting one unit face from every cluster of four and intersecting them, obtaining a "modified" TOS block, as seen in Fig. 13.

To obtain hexagonal blocks, we consider the diagonal on each of the 6 new contact faces on a block, then define a plane that passes approximately through their midpoints (mid-plane). Finally, we offset this plane to obtain two parallel truncation planes defining the intrados and extrados of the block, as seen in Fig. 14. The offset distances of the truncation planes vary so as to reduce the overall weight and material waste while maintaining the overall stability of the structure.

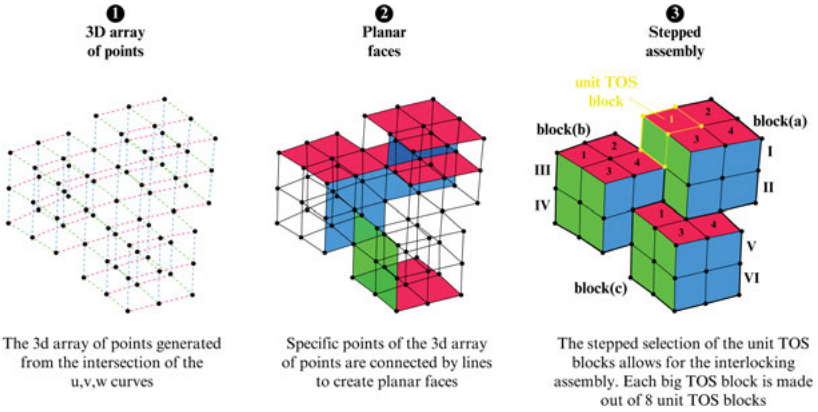

Fig. 12: Big TOS blocks (clusters of 8 units).

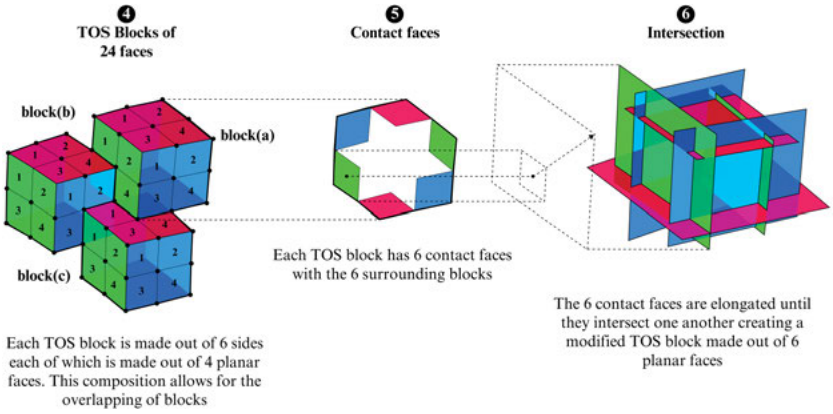

Fig. 13: Generating TOS blocks of 6 faces.

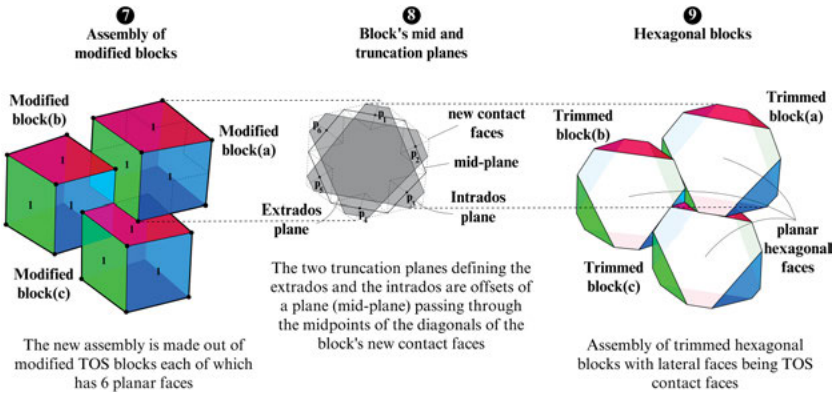

Fig. 14: Obtaining hexagonal blocks.

The version of the TOS interlocking system presented above was developed jointly with Maurizio Brocato and Paul Nougayrède of the GSA lab as a pre-rationalized approach to the design and construction of doubly curved stone structures.

5 Conclusion

In the article, we presented a geometric setting, namely the TOS, with clear advantages for architectural design and fabrication. Next, we established a design model which articulated viable ways of creating a search space for morphological options and parameters to manipulate it at the block level while remaining true to the initial geometry. Finally, we showed how once a morphological option is chosen though the 5 DF, it is translated into a design prototype, namely a stone vault from an interlocking system arising from the TOS. Hence, setting the ground for the next phase of this research, where the parameters that went into the conception of this prototype are highlighted.

Acknowledgments

The research of Elshafei, A. was partially financed by Portuguese Funds through FCT (Fundação para a Ciência e a Tecnologia) within the Projects UIDB/00013/2020 and UIDP/00013/2020. The research of Tošić, Z. is a part of the priority program SPP 2187: Adaptive Modular Construction with Flow Production Methods – Precision High-Speed Construction of the Future in the subproject Formwork-free Flow Production of Adaptive Supporting Structures from Variable Frame Elements – Adaptive Concrete Diamond Construction (ACDC) funded by the German Research Foundation (DFG).

References

Abdelmagid, A., A. Elshafei, M. Mansouri, and A. Hussein. (2022). A design model for a (grid)shell based on a triply orthogonal system of surfaces. In *Towards Radical Regeneration: DMS Berlin*.

Bobenko, A. and S. Tsarev. (2007). Curvature line parameterization from circle patterns. https://arxiv.org/abs/0706.3221

Brocato, M. and L. Mondardini. (2010). Geometric methods and computational mechanics for the design of stone domes based on abeille's bond. In *Advances in Architectural Geometry 2010*.

Cecil, T. E. (2018). Lie sphere geometry and dupin hypersurfaces. *Mathematics Department Faculty Scholarship*.

Eisenhart, L. (1909). *A treatise on differential geometry of curves and surfaces*. Ginn and Company, Boston.

Gray, A., E. Abbena, and S. Salamon. (2006). Modern differential geometry of curves and surfaces with Mathematica. 3rd Edition. Chapman & Hall/CRC.

Liu, Y., H. Pottmann, J. Wallner, Y. Yang, and W. Wang. (2006). Geometric modeling with conical meshes and developable surfaces. *ACM Tr., Proc. SIGGRAPH,* 25(3): 681–89.